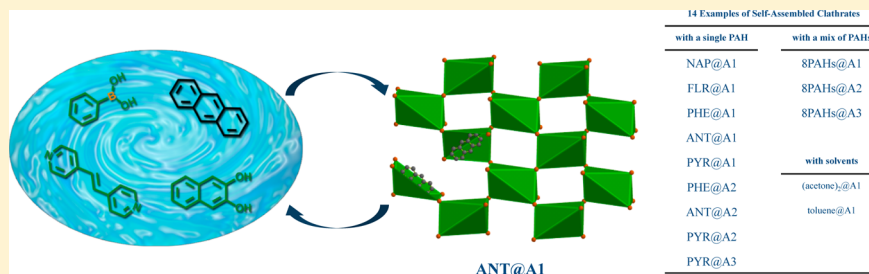


Selective Isolation of Polycyclic Aromatic Hydrocarbons by Self-Assembly of a Tunable N→B Clathrate

Angel D. Herrera-España,[†] Gonzalo Campillo-Alvarado,[†] Perla Román-Bravo,[†] Dea Herrera-Ruiz,[‡] Herbert Höpfl,[†] and Hugo Morales-Rojas^{*†}[†]Centro de Investigaciones Químicas, and [‡]Facultad de Farmacia, Universidad Autónoma del Estado de Morelos, Av. Universidad 1001, C.P. 62209 Cuernavaca, Morelos, México

S Supporting Information



ABSTRACT: The combination of one dipyrindyl linker [1,2-di(4-pyridyl)ethylene (DPE), 1,2-di(4-pyridyl)ethane (DPeT), or 4,4'-azopyridine (DPA)] with two molecules of arylboronate ester **1** produced dinuclear Lewis-type N→B adducts that can act as acyclic host for polycyclic aromatic hydrocarbons (PAHs) in the solid state. Nine crystalline solids of composition PAH@adduct (i.e., one PAH per adduct) were obtained from solutions containing a single PAH. On the basis of the single-crystal X-ray diffraction analysis of the compound ANT@A1 (ANT = anthracene; A1 = adduct being composed of DPE and two boronate esters **1**), the PAH inclusion selectivity is related to a size-fitting adaptation to an octahedral-shaped pocket assembled by CH- π interactions between fragments of the diamine and the arylboronate ester **1**. The resulting reversible organic clathrates can perform “catch and release” cycles of PAHs such as pyrene and can sequester selectively PAHs from mixtures in solution.

The molecular recognition of polycyclic aromatic hydrocarbons (PAHs) is a challenging issue given the variety of sizes, shapes, and properties of these widespread materials.¹ PAHs are among the most intensively studied pollutants in the environmental analysis of air, water, food, and solid-waste samples. Methods for quantitative separation and detection of PAHs often rely on traditional chromatographic and solvent-extraction protocols.² A well-established supramolecular approach to bind PAHs in solution consists of the use of polycationic macrocycles and cages derived from extended viologens, which are assembled covalently³ or through metal coordination.⁴ The association constants of these host-guest complexes in water and polar solvents range between 10¹ and 10⁶ M⁻¹, and a significant number of X-ray crystal structures of such complexes has been reported. Yet these elegant supramolecular receptors were made in multistep synthetic procedures³ or involved costly transition metals.⁴ Thus, it is still a demanding task to develop simple methods to selectively detect PAHs, and also to be able to recover them quantitatively as a single (or multiple) PAH from mixtures in solution.^{1,2}

In the past decade, various research groups have comprehensively explored the interaction of aromatic amines with boronate esters and boroxines to provide a broad variety of discrete and polymeric materials, such as macrocycles,⁵ nanostructures,⁶ coordination polymers,⁷ and gels.⁸ Hence, supramolecular assembly based on dative N→B interactions is

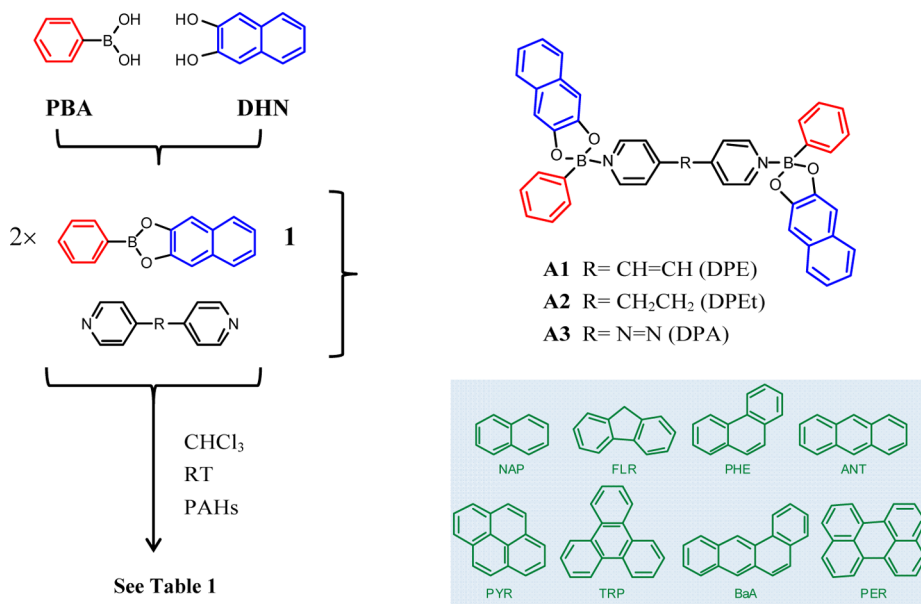
recognized as a useful strategy for the generation of complex systems, and given its thermodynamic stability (−11 to −38 kJmol⁻¹)^{6,7} and kinetic lability in polar coordinating solvents, the central N→B binding motif can be compared to a typical noncovalent interaction. The potential of this approach is well exemplified by the prismatic organic cages assembled via N→B bonds that were able to encapsulate triphenylene or coronene in the solid state.^{6c} These previous reports have also evidenced that simple arylmonoboronate esters normally form 2:1 Lewis-type adducts in the presence of diamines such as 4,4'-bipyridine (BiPY) or 1,2-di(4-pyridyl)ethylene (DPE).⁷ As a consequence, the dipyrindyl aromatic moieties become electron-deficient, and because of being embedded in a tweezer-type arrangement, they might become suitable to recognize electron-rich species. Since a systematic search about the prospects of these discrete species to act as acyclic molecular host for PAHs is still missing, this turned on our interest in exploring the supramolecular chemistry between discrete N→B adducts and electron-rich PAHs.

Herein, we report the first example of a family of discrete tweezer-type N→B adducts that starting from three or four molecular components assemble into solid-state clathrates⁹

Received: February 12, 2015

Published: February 26, 2015

Scheme 1. Molecular Components Used to Assemble N→B Adducts Containing PAHs as Crystalline Solids



with inclusion of PAHs. Initial condensation of phenylboronic acid (PBA) and 2,3-dihydroxynaphthalene (DHN) in acetonitrile gave boronate ester **1** in good yields (Scheme 1). Upon stirring a chloroform solution containing **1** and DPE in a 2:1 molar concentration ratio for 1 h at RT, a solid precipitated that could be isolated by filtration (**A1**, 91%). **A1** presented a powder X-ray diffraction (PXRD) pattern different from that of the starting materials (Figure 1a–c) and the NMR spectro-

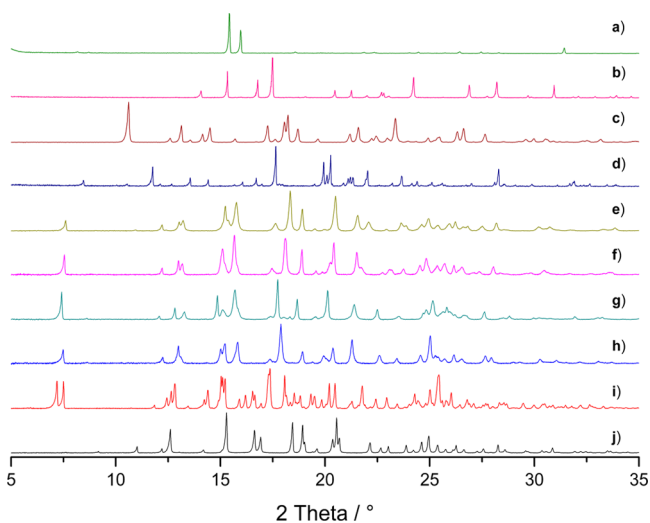


Figure 1. PXRD patterns from top to bottom: (a) **1**; (b) DPE; (c) **A1**; (d) (acetone)₂@**A1**; (e) NAP@**A1**; (f) FLR@**A1**; (g) PHE@**A1**; (h) ANT@**A1**; (i) PYR@**A1**; (j) toluene@**A1**.

scopic analysis in DMSO-*d*₆ showed signals for both **1** and DPE in the expected 2:1 ratio (Figure S1, Supporting Information (SI)). Adduct **A1** could also be isolated by performing the reaction in refluxing acetone starting from a multicomponent mixture of PBA, DHN, and DPE in a 2:2:1 ratio, conditions that point out that *in situ* formation of the boronate ester **1** is achieved easily.

By lowering temperature of the above-described mixture in acetone to 6 °C, a novel crystalline solid precipitated, that

according to the thermogravimetric analysis (TGA) resulted to be the acetone solvate of **A1** (Figure S2, SI). Single-crystals suitable for X-ray diffraction analysis could be grown from acetone at *T* < 6 °C that evidenced the suggested molecular composition and the presence of dative N→B bonds (Figure 2 and Figure S3, SI). In the crystal lattice, the boron atoms are four-coordinated with a tetrahedral character (THC)¹⁰ of 79.6% and N→B bond lengths of 1.6321(18) Å. Two molecules of acetone are included per **A1** adduct, which are confined in pockets generated by the phenyl and naphthoyl substituents of the boronate ester and bound through CH_{acetone}⋯π and CH_{pyridyl}⋯O_{acetone} interactions (Figure 2c,d).

After this promising result, a systematic screening was performed in order to evaluate if PAHs can be also included (PAHs used: naphthalene (NAP), fluorene (FLR), phenanthrene (PHE), anthracene (ANT), pyrene (PYR), triphenylene (TRP), benzo(a)anthracene (BaA), and perylene (PER); see structures in Scheme 1). Stirring of **1**, DPE and the corresponding PAH in a 2:1:1 molar ratio in chloroform solution at RT for 1 h afforded new crystalline solids in the presence of NAP, FLR, PHE, ANT, and PYR (Table 1), respectively, that were isolated by simple filtration of the reaction product. Each of these solids showed an entirely different diffraction pattern when compared to **A1** or the starting materials (see Figure 1e–i). Notably, the diffraction patterns are quite similar and display a characteristic peak around $2\theta = 7.5^\circ$. As representative example, ANT@**A1** was assembled also in 48% yield in CHCl₃ from a four-component mixture of PBA, DHN, DPE, and ANT in a 2:2:1:1 ratio. The lability of both the N→B and B–O bonds in aqueous methanolic solutions enables to dissociate all of these solids again into the starting components, as shown by HPLC analysis, which allowed us to identify and to quantify individually PBA (as the methyl ester), DHN, DPE, and the corresponding PAH (see Table S1 and Figure S4, SI).¹¹ Composition of these solids was found having the same stoichiometric ratio PBA/DHN/DPE/PAH (2:2:1:1), indicating a general composition of **A1**/PAH (1:1).

Compound ANT@**A1** crystallized as orange blocks that displayed fluorescence under UV-light (see Figure S5a, SI) and

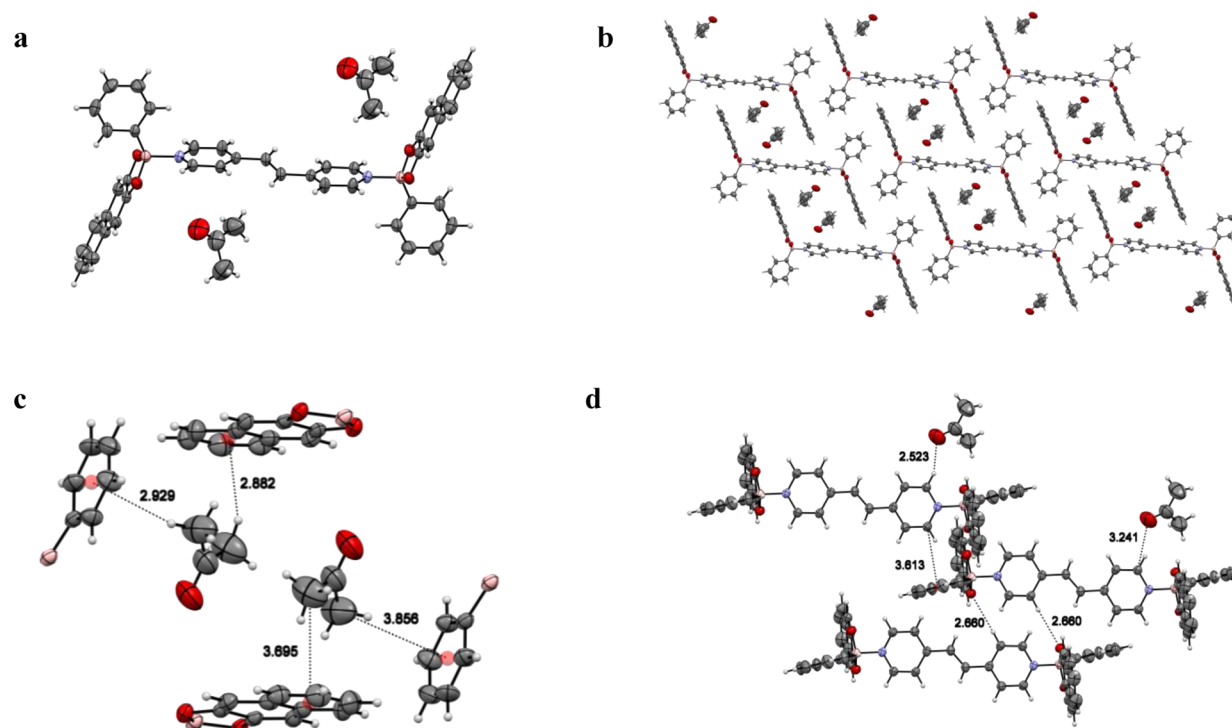


Figure 2. X-ray structure of (acetone)₂@A1. (a) Asymmetric unit; (b) view along the *ac* plane that shows the relative orientation of the acetone guest molecules; (c) CH_{acetone}... π interactions; (d) CH_{pyridyl}...O_{acetone} and CH_{pyridyl}...O_{boronate} interactions. Distances are in angstroms.

Table 1. Results of the Screening Experiments for the Formation of Clathrate Compounds from Combinations of 1 with Dipyrindyl Linkers^d

	NAP ^a	FLR ^a	PHE ^a	ANT ^a	PYR ^a	TRP ^a	BaA ^a	PER ^a
	<i>L</i> = 9.195, <i>B</i> = 7.428 <i>L/B</i> = 1.238	11.43, 7.521 1.520	11.75, 8.031 1.463	11.65, 7.434 1.566	11.66, 9.279 1.257	11.68, 10.44 1.119	13.94, 8.717 1.599	11.80, 9.247 1.276
DPE^b	✓ NAP@A1	✓ FLR@A1	✓ PHE@A1	✓ ANT@A1	✓ PYR@A1	✗	✗	✗
<i>L</i> = 12.388	2.6 ^c	4.5 ^c	3.3 ^c	3.6 ^c	2.1			
<i>B</i> = 7.889	Yellow	Yellow	Yellow	Orange & F	Pale-Orange & F			
<i>L/B</i> = 1.570								
DPEt^b	✗	✗	✓ PHE@A2	✓ ANT@A2	✓ PYR@A2	✗	✗	✗
12.309			6.1 ^c	6.0 ^c	5.1 ^c			
8.052			White	White & F	White			
1.529								
DPA^b	✗	✗	✗	✗	✓ PYR@A3	✗	✗	✗
11.911					4.3 ^c			
7.917					Dark-red			
1.504								

^aStructural parameters for PAHs molecules are shown below the three letter code corresponding to the maximum dimensions in angstroms for the length (*L*), breadth (*B*), and *L/B* ratio according to the Polycyclic Hydrocarbon Structure Index NIST special publication 922. ^bStructural parameters *L*, *B*, and *L/B* ratio for dipyrindyl molecules are shown and were calculated using the Spartan'10 software package. ^cSolubility of the solids in CHCl₃ at 25 °C; value is given in mM concentration units. All solids remained stable during the elapsed time of these experiments (3 h) as indicated by the corresponding PXRD analyses. ^dGreen check mark: A new crystalline solid precipitated out from solution. Color under ambient light and fluorescence (F) under UV light exposure is also indicated. Red X-marks: No precipitate was observed or just the adduct A1 or A2 was recovered.

was further examined by single-crystal X-ray diffraction analysis.¹² The crystal lattice is essentially built up by interactions between the A1 adducts, in which the fragments from 1 and DPE play different roles. The DPE fragments embed the ANT molecules in a sandwich-like manner into infinite π - π stacked pillars along the *a* axis (Figure 3a,b, green/blue CPK) with centroid...centroid distances ranging from 3.52 to 3.87 Å.

The boronate ester fragments from neighboring A1 adducts (Figure 3a,b red stick) complete the ensemble by joining the DPE fragments via three CH... π interactions, giving octahedral-shaped pockets containing the ANT guest (Figure 3d).

Interestingly, there are no appreciable intermolecular interactions with the guest molecules other than van der Waals contacts. This organization indicates a cooperative process between the adduct components to build up a pocket that comfortably accepts ANT (*L* = 11.65 Å, *B* = 7.43 Å, *L/B* = 1.57). The same framework must be present in the other inclusion compounds given the similarity of the PXRD patterns, and therefore these pockets are endowed with some adaptability, which allows for the inclusion of other PAHs within a size range of *L* = 9.20–11.75 Å, *B* = 7.43–9.28 Å and *L/B* = 1.24–1.52 (i.e., NAP, FLR, PYR, and PHE). Longer or

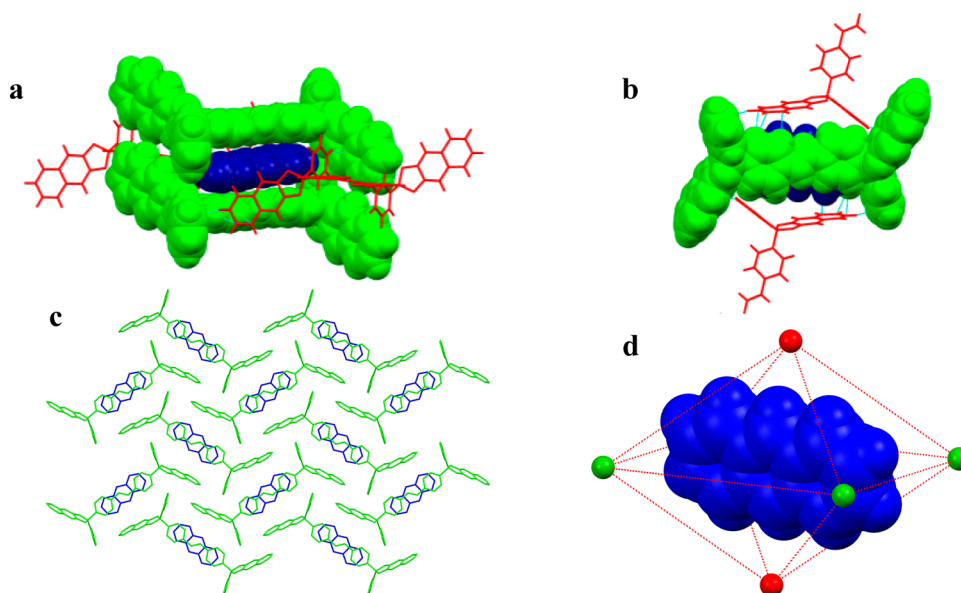


Figure 3. X-ray structure of ANT@A1. Panels (a) and (b) display different views of the A1 ensemble that includes ANT. (c) View of the *bc* plane showing the relative orientation of the ANT guest molecules. (d) Boron atoms forming an octahedral-shaped pocket containing ANT.

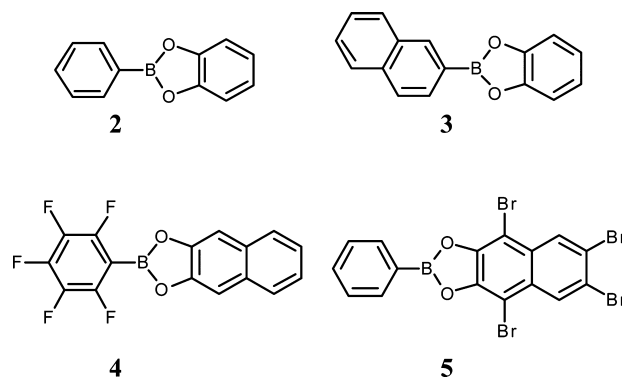
broader PAHs, such as BaA, PER, or TRP (see Table 1), did not afford inclusion compounds under these conditions.

To further test of these structural features, screening experiments with PHAs were also performed with mixtures of **1** and 1,2-di(4-pyridyl)ethane (DPeT), 4,4'-azopyridine (DPA) or 4,4'-bipyridine (BiPy). In the absence of PAHs, the 2:1 adduct **A2** (1:DPeT) precipitated as an inclusion complex with DHN, whereas the adduct **A3** (1:DPA) was obtained as a homogeneous solid (see Figures S5b, S5c, S7, and S8, SI). Solutions of **1** with BiPy in CHCl₃ remained without precipitates, but in the presence of a single PAH just the 2:1 adduct 1:BiPy was recovered. However, from solutions of **1**, DPeT, and a single PAH, three cocrystalline solids having the composition A2/PAH (1:1) were formed with ANT, PHE, and PYR. With DPA, only one solid precipitated (with PYR) with the composition A3/PYR (1:1) (see Table 1, Figures S7 and S8, SI).

Since the diamines DPE, DPeT, and DPA hold a similar length (see Table 1), it seems that the nature of the diamine linker plays an essential role and changes the selectivity of the crystallization-induced formation of these clathrates in chloroform solutions, indicating that electronic complementarity is also required, particularly, for the smaller PAH guests such as NAP or FLR.

Screening experiments using other boronate esters (**2–5**), DPE and a single PAH produced mostly only the corresponding 2:1 adducts, without inclusion of the PAH, emphasizing the importance of the right orientation, size, and the availability of C-H atoms to arrange the recognition pocket.

Finally, a couple of experiments were carried out to test the feasibility of applications for the 1-DPE/DPeT/DPA systems. First, an equimolar solution containing all eight PAHs included in this study (0.2 mmol each) was stirred with **1** (0.4 mmol) and 1 equiv of the dipyridyl linker (0.2 mmol of DPE, DPeT, or DPA) in chloroform. Solids precipitated after 1 h and showed a PXRD pattern that resemble those corresponding to the solids isolated from the experiments with single PAHs (Figure S9, SI). The HPLC traces of the PAHs released from these solids in aqueous methanol are depicted in Figure S10a,b, and the data



are summarized in Table S2. Rather than a single PAH, the three multicomponent solids collected a varying distribution of PAHs. PYR and PHE were present in all three systems and were also the most abundant guests, comprising 60–70% of the PAHs removed from the solution mixture. Unusually, PAHs that formerly did not precipitate from a single component solution (i.e., TRP, BaA, and PER) were also found in the solid mixture although in minor quantities. Of the adducts, **A1** was the most promiscuous, incorporating all PAHs with quantities in the following order PYR > PHE > ANT ≫ PER > FLR ~ NAP > BaA > TRP. **A3** was the most selective clathrate, leaving out NAP, ANT, and BaA, and increasing twice the relative amount of PYR incorporated in the lattice. Therefore, the distribution of PAHs in these solids is not driven solely by their intrinsic solubility with values in the mM range (Table 1). For instance, PYR@A1 is the less soluble inclusion compound, and therefore, it is expected to dominate in the mixture. However, NAP is present 7-fold less than PYR in 8PAHs@A1 or 8PAHs@A, albeit NAP@A1 is slightly more soluble (2.1 mM vs 2.6 mM, PYR vs NAP). In the same context, PHEN and ANT were included in these solids at a constant 3:2 ratio in spite of their similar solubility.

In a second experiment, solid toluene@A1¹³ (100 mg, 0.130 mmol) was added to a PYR solution in CHCl₃ (2 mL, 68 mM) and its color changed immediately from yellow to orange. After this mixture was stirred for 1 h, the solid was removed by

filtration giving 98 mg of the compound PYR@A1, thus removing 88% of the PYR present in the initial solution (Figure S11). This latter solid (98 mg) was suspended in 3 mL of toluene and heated up to 100 °C for 1 h. The insoluble material was removed by filtration giving 68 mg of the starting solvate toluene@A1 with no trace of PYR@A1 according to the PXRD analysis (Figure S11, SI). Thus, as determined from the toluene filtrate by UV–vis spectroscopy, PYR was fully released back into solution.

In conclusion, for the first time a series of reversible organic clathrates assembled in one-step that can incorporate a single or a blend of PAHs into crystalline solids at RT is described. In these solids, recognition pockets are built by the cooperative assembly based on the combination of an arylboronic acid, a diol (or the corresponding boronate ester **1**), and a suitable diamine linker into N→B adducts (i.e., A1), which are further linked through CH $\cdots\pi$ interactions forming an octahedral-shaped cavity. A strategy for the reversible “catch and release” of PAHs under mild conditions has been projected. We envision that a combination of other di- or oligoamine connectors and suitable arylboronic esters might provide the required complementary sites toward heavier PAHs as well as other aromatic heterocycles.

■ ASSOCIATED CONTENT

Supporting Information

Synthetic procedures and spectroscopic analyses, TGA, PXRD and HPLC data. This material is available free of charge via the Internet at <http://pubs.acs.org>.

■ AUTHOR INFORMATION

Corresponding Author

*Fax: (+52) 77-73-29-79-97. E-mail: hugom@uaem.mx.

Notes

The authors declare no competing financial interest.

■ ACKNOWLEDGMENTS

This work was supported by Consejo Nacional de Ciencia y Tecnología (CONACyT) through Project No. CB2009-132227. The authors gratefully acknowledge for awarding access to the instrumental facilities in the Chemical Research Center at the Autonomous State University of Morelos (CIQ-UAEM).

■ REFERENCES

- (1) (a) Harvey, R. G. *Polycyclic Aromatic Hydrocarbons*; Wiley-VCH: New York, 1997. (b) Lehn, J.-M. *Supramolecular Chemistry Concepts and Perspectives*; Wiley-VCH: Weinheim, Germany, 1995. (c) Atwood, J. A.; Steed, J. W. *Supramolecular Chemistry*; Wiley-VCH: Weinheim, Germany, 2009.
- (2) (a) Raters, M.; Matissek, R. *J. Agric. Food Chem.* **2014**, *62*, 10666. (b) Purcaro, G.; Moret, S.; Lanfranco, S. C. *Talanta* **2013**, *105*, 292. (c) Wenzl, T.; Simon, R.; Anklam, E.; Kleiner, J. *Trends Anal. Chem.* **2006**, *25*, 716.
- (3) (a) Barnes, J. C.; Juriček, M.; Strutt, N. L.; Frascioni, M.; Sampath, S.; Giesener, M. A.; McGrier, P. L.; Bruns, C. J.; Stern, C. L.; Sarjeant, A. A.; Stoddart, J. F. *J. Am. Chem. Soc.* **2013**, *135*, 183. (b) Juriček, M.; Barnes, J. C.; Dale, E. J.; Liu, W.; Strutt, N. L.; Bruns, C. J.; Vermeulen, N. A.; Ghooray, K. C.; Sarjeant, A. A.; Stern, C. L.; Botros, Y. Y.; Goddard, W. A., III; Stoddart, J. F. *J. Am. Chem. Soc.* **2013**, *135*, 12736. (c) Dale, E. J.; Vermeulen, N. A.; Thomas, A. A.; Barnes, J. C.; Juriček, M.; Blackburn, A. K.; Strutt, N. L.; Sarjeant, A. A.; Stern, C. L.; Denmark, S. E.; Stoddart, J. F. *J. Am. Chem. Soc.* **2014**, *136*, 10669. (d) Hafezi, N.; Holcroft, J. M.; Hartlieb, K. J.; Dale, E. J.; Vermeulen, N. A.; Stern, C. L.; Sarjeant, A. A.; Stoddart, J. F. *Angew. Chem., Int. Ed.* **2015**, *54*, 456.
- (4) (a) Peinador, C.; Pía, E.; Blanco, V.; García, M. D.; Quintela, J. M. *Org. Lett.* **2010**, *12*, 1380. (b) Blanco, V.; García, M. D.; Terenzi, A.; Pía, E.; Fernández-Mato, A.; Peinador, C.; Quintela, J. M. *Chem. Eur. J.* **2010**, *16*, 12373. (c) Alvaríño, C.; Pía, E.; García, M. D.; Blanco, V.; Fernández, A.; Peinador, C.; Quintela, J. M. *Chem. Eur. J.* **2013**, *19*, 15329.
- (5) (a) Christinat, N.; Scopelliti, R.; Severin, K. *Chem. Commun.* **2004**, 1158. (b) Severin, K. *Dalton. Trans.* **2009**, 5254. (c) Sheepwash, E.; Zhou, K.; Scopelliti, R.; Severin, K. *Eur. J. Inorg. Chem.* **2013**, 2558.
- (6) (a) Christinat, N.; Scopelliti, R.; Severin, K. *J. Org. Chem.* **2007**, *72*, 2192. (b) Christinat, N.; Scopelliti, R.; Severin, K. *Angew. Chem., Int. Ed.* **2008**, *47*, 1848. (c) Icli, B.; Sheepwash, E.; Riis-Johannessen, T.; Schenk, K.; Filinchuk, Y.; Scopelliti, R.; Severin, K. *Chem. Sci.* **2011**, *2*, 1719. (d) Christinat, N.; Scopelliti, R.; Severin, K. *Chem. Commun.* **2008**, 3660.
- (7) (a) Salazar-Mendoza, D.; Cruz-Huerta, J.; Höpfl, H.; Hernández-Ahuactzi, I. F.; Sanchez, M. *Cryst. Growth Des.* **2013**, *13*, 2441. (b) Cruz-Huerta, J.; Salazar-Mendoza, D.; Hernández-Paredes, J.; Hernández-Ahuactzi, I. F.; Höpfl, H. *Chem. Commun.* **2012**, *48*, 4241. (c) Salazar-Mendoza, D.; Guerrero-Alvarez, J.; Höpfl, H. *Chem. Commun.* **2008**, 6543. (d) Icli, B.; Solari, E.; Kilbas, B.; Scopelliti, R.; Severin, K. *Chem. Eur. J.* **2012**, *18*, 14867. (e) Sheepwash, E.; Luisier, N.; Krause, M. R.; Noé, S.; Kubik, S.; Severin, K. *Chem. Commun.* **2012**, *48*, 7808. (f) Christinat, N.; Croisier, E.; Scopelliti, R.; Cascella, M.; Röthlisberger, U.; Severin, K. *Eur. J. Inorg. Chem.* **2007**, 5177.
- (8) (a) Luisier, N.; Schenk, K.; Severin, K. *Chem. Commun.* **2014**, 50, 10233. (b) Ito, S.; Takata, H.; Ono, K.; Iwasawa, N. *Angew. Chem., Int. Ed.* **2013**, *52*, 11045. (c) Sheepwash, E.; Krampfl, V.; Scopelliti, R.; Sereda, O.; Neels, A.; Severin, K. *Angew. Chem., Int. Ed.* **2011**, *50*, 3034.
- (9) For selected examples of purely organic clathrates as host–guest systems see: (a) Lee, J. J.; Sobolev, A. N.; Turner, M. J.; Fuller, R. O.; Iversen, B. B.; Koutsantonis, G. A.; Spackman, M. A. *Cryst. Growth Des.* **2014**, *14*, 1296. (b) Natarajan, P.; Bajpai, A.; Venugopalan, P.; Moorthy, J. N. *Cryst. Growth Des.* **2012**, *12*, 6134. (c) le Roex, T.; Nassimbeni, L. R.; Weber, E. *Chem. Commun.* **2007**, 1124. (d) Curtis, E.; Nassimbeni, L. R.; Su, H.; Taljaard, J. H. *Cryst. Growth Des.* **2006**, *6*, 2716.
- (10) Höpfl, H. *J. Organomet. Chem.* **1999**, *581*, 129.
- (11) HPLC = high performance liquid chromatography. Because of the limited solubility and dynamics of these adducts in solution, it was not possible to accurately measure the composition by NMR spectroscopy, but the 1:1 composition was confirmed by elemental analysis for ANT@A1 (see SI).
- (12) Crystal data for [(acetone)₂@A1] (CCDC 1040427); C₄₄H₃₂B₂N₂O₄·(C₃H₆O)₂; M_r = 790.49, 0.553 × 0.333 × 0.188 mm³, triclinic, space group P $\bar{1}$, a = 9.0771(3) Å, b = 10.8773(3) Å, c = 11.3414(4) Å, α = 77.9240(10)°, β = 81.0780(10)°, γ = 76.8330(10)°, V = 1059.41(6) Å³, Z = 1, r_{calc} = 1.239, T = 298 K, 2 θ _{range} = 1.955 to 25.404°. 12558 reflections measured, 3867 unique (R_{int} = 0.0312), R₁ = 0.0446 for 3191 reflections with I > 2 σ (I) and wR₂ = 0.1231 for all data, 309 parameters, GOF = 1.036. (b) Crystal data for [ANT@A1] (CCDC 1040428); C₄₄H₃₂B₂N₂O₄·(C₁₄H₁₀); M_r = 852.55, 0.455 × 0.148 × 0.097 mm³, monoclinic, space group P2₁/c, a = 7.3455(3) Å, b = 20.4878(9) Å, c = 14.8292(7) Å, α = 90°, β = 103.6060(10)°, γ = 90°, V = 2169.06(17) Å³, Z = 2, r_{calc} = 1.305, T = 298 K, 2 θ _{range} = 1.727–25.361°. 12584 reflections measured, 3964 unique (R_{int} = 0.0358), R₁ = 0.0458 for 2594 reflections with I > 2 σ (I) and wR₂ = 0.1252 for all data, 299 parameters, GOF = 1.17.
- (13) Toluene@A1 could be isolated either from a multicomponent mixture of PBA, DHN, and DPE in toluene under reflux or by combination of the boronate ester **1** and DPE at RT (ca. 95% yield; see PXRD pattern Figure 1j). The 1:1 composition of was established by thermogravimetric analysis (Figure S2, SI).